Computational Investigation of Flame Acceleration and Transition to Detonation

Nolan Dexter-Brown, Jagannath Jayachandran*
Worcester Polytechnic Institute
Worcester, MA, USA

1 Introduction

The phenomenon of detonation formation has been extensively discussed since its identification in the late 1880s. Despite more than a century of research, the mechanisms underlying the deflagration-to-detonation transition (DDT) in semi- and unconfined systems remain a subject of active debate. The necessity for predicting the onset of DDT is becoming increasingly important, particularly in light of the transition towards a clean, hydrogen-based fuel economy. This is emphasized by the high detonability of hydrogen-air mixtures and the resulting sharp pressure gradients across detonation fronts. Furthermore, detonations offer potential applications in highly efficient power cycles [1], and they play a critical role in the explosions of type Ia supernovae [2]. A detailed understanding of detonation formation is required to ensure safe storage and handling of H_2 and reliably operating engines.

During the past four decades, several mechanisms for DDT have been proposed [2–15]. Shchelkin and Troshin attributed DDT to the formation of an auto-ignition center resulting from strong shocks preceding accelerating flames [3]. Zel'dovich argued that gradients in ignition delay (temperature) allowed for the coupling of heat release and pressure waves, facilitating detonation formation. Lee et al. presented a similar theory on shock wave amplification by coherent energy release (SWACER) [5]. Liberman and colleagues observed that during the final stages of runaway towards DDT, coupling occurs between increasing pressure and heat release rate [6–9]. This positive feedback results in pressure buildup within the flame, driving flame acceleration until detonation onset. Poludnenko and coworkers proposed a similar theory for turbulent flames, stating that energy (pressure) accumulation occurs once the turbulent flame speed exceeds the Chapman-Jouguet deflagration velocity; the steady-state flame structure is disrupted, driving spontaneous detonation formation [2, 10]. Deshaies and Joulin [11] and then Clavin [12] proposed that increased flame area results in increased burned gas flow towards the flame tip, which acts as a piston accelerating the flame brush. The resulting acceleration continues until a shock forms within the flame, blowing up the inner structure and forming a detonation [12–15]. Various experimental studies have shown the presence of pressure accumulation locally ahead of the flame prior to DDT [2, 16].

Experimental studies are fundamentally limited in its ability to elucidate the mechanism of DDT. This is due to the stochastic nature of the process and the limited number of simultaneous measurements that are feasible. Direct numerical simulations (DNS) provide the entire flow field for a detailed analysis

Correspondence to: jjayachandran@wpi.edu

[2, 6–10, 17, 18]. Prior investigations implemented minimum grid spacing on the order of 20 microns, with the smallest being 3.5 microns by [17, 18]. From our analysis, it appears that these resolutions were chosen to resolve the flame structure prior to flame acceleration and not immediately prior to DDT. These studies do not discuss the ability of the simulations to accurately capture the flame structure and evolution just prior to DDT. Resolving the flame for all times is critical to ascertain the mechanisms controlling DDT, especially if the mechanism involves pressure buildup within the flame.

The purpose of this study is to probe the final stages of flame acceleration and DDT using numerical simulations to probe and elucidate the underlying mechanisms. Consequently, we perform 2-D DNS while attempting to resolve the flame structure at all times prior to flame runaway and DDT. Note that the focus was on understanding how an increase in flame area affects pressure gain and modification of the flame structure. We do not attempt to completely resolve the wall boundary layer ahead of the flame, which is known to drive the increase in flame area, and requires 3-D simulations to accurately capture all the relevant (turbulent) scales (computationally prohibitive!). The results presented shed light on the role of coupling between flame area growth and how it affects the burned gas velocity and pressure buildup at the tip of elongated finger-like flames prior to DDT. Additionally, simulations show that for the case studied, transition occurs through the pressure build-up within the laminar flame as first discussed by Liberman et al. [6] and by Clavin and coworkers [12–15].

2 Numerical Methods

Numerical simulations are performed using PeleC [19], an open-source code that solves the conservative form of the conservation equations and built upon the block-structured adaptive mesh refinement (AMR) framework of AMReX. Two-dimensional simulations are conducted within a 284 cm long channel with a width of 0.09 cm at an initial temperature (T_o) and pressure (P_o) of 503 K and 10 bar, similar to Yang. et al. [17]. Choices of the 2-D (vs. 3-D) simulation and small channel width were made to enable reasonably resolved simulations at affordable computational cost. The domain boundaries include no-slip lateral walls and solid left and zero-slope right vertical boundaries. A schematic of the simulation domain is displayed in Fig. 1. The base grid for all simulations spans 51200 by 16 (819200) cells. A detailed chemical kinetic model with nine species (H_2, O_2, H_2O, H, O, OH, HO_2, H_2O_2, and N_2) and 21 reactions developed by Li et al. [20] was used.

Grid refinement is handled by AMReX, which increases the number of cells present through, $\Delta x_o/\Delta x_\mathrm{n} = 2^\mathrm{n}$. Δx_o is the base level zero grid resolution, Δx_n is the current level resolution, and n is the current level. Changes in temperature between adjacent cells (10 K) were utilized as a criterion for refinement, while the maximum extent of refinement was controlled by the maximum allowable grid level. For all spatial resolutions investigated, the number of grid cells within the flame was compared at t = 0 ($T_\mathrm{o} = 503$ K, $P_\mathrm{o} = 10$ bar) and at the beginning of the transient flame evolution regime t ≈ 2.4 ms ($T(t = 2.4\,\mathrm{ms}) = 753$ K, $P(t = 2.4\,\mathrm{ms}) = 43.4$ bar), see Table 1. Flame thickness (δ_f) was calculated using the maximum temperature gradient method [21] of fully resolved flame simulations using Cantera.

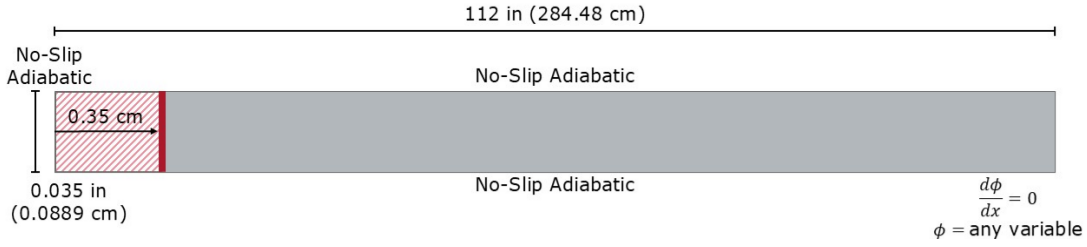

Figure 1: Schematic of the 2-D simulation domain.

Simulations are initialized with a 1-D freely propagating premixed flame from Cantera. This solution profile is then imposed onto a planar sheet near the left boundary of the domain. Initially, the system is at rest with constant pressure throughout and then allowed to evolve in time, with the flame propagating to the right until DDT is observed.

Table 1: Simulation grid refinement maximum level with corresponding spatial resolution and number of computational cells across the flame at $t = 0$ and $t \approx 2.4$ ms.

Level	Grid Resolution [μm]	Grid Cells Across Flame	
		$t = 0$	$t \approx 2.4$ ms
3	6.95	2.2	0.4
4	3	3	0.9
5	1.74	8.7	1.7
6	0.87	17.4	3.3

3 Results

Combustion in semi-confined environments results in the development of an induced flow in the direction of flame propagation due to the expansion of hot products. Flame acts like a porous piston pushing and accelerating the gas ahead of it. This produces pressure waves that originate on the piston head (burned gas flow) and propagate downstream. After some time, these pressure waves can coalesce, forming shocks far ahead of the flame, adiabatically compressing and heating the reactants entering the flame (T_f, P_f), resulting in a higher burning flux. This cycle repeats until runaway and DDT occurs [6–8, 12, 16].

The evolution of flames in channels can be divided into two major phases: quasi-steady and transient. Figure 2a displays the overall time evolution of flame area (A_f), unburned and burned gas velocity (u_uf and u_bf), and the pressure of the reactants entering the flame (P_f). The quasi-steady regime is noted by the region of constant flame acceleration ($t \lesssim 2.4$ ms). During this phase, the rate of flame acceleration is low enough that generated pressure waves have sufficient time to propagate far ahead of the flame. Figure 3a displays the velocity and pressure fields from simulations during the quasi-steady phase ($t =$

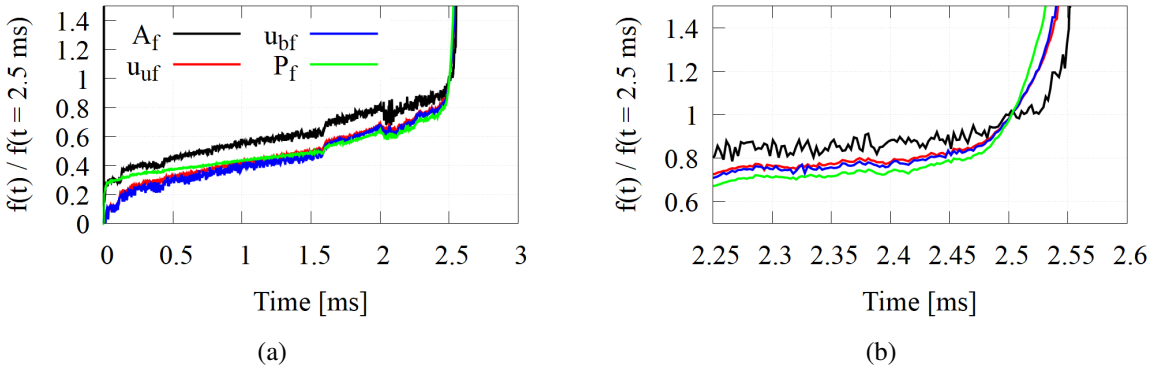

Figure 2: Temporal evolution of the flame area (A_f), unburnt and burnt gas velocities (u_uf and u_bf), and pressure adjacent ahead of the flame (P_f) (a) throughout the entire simulation and (b) during the runaway process. Values are scaled by the value at 2.5 ms.

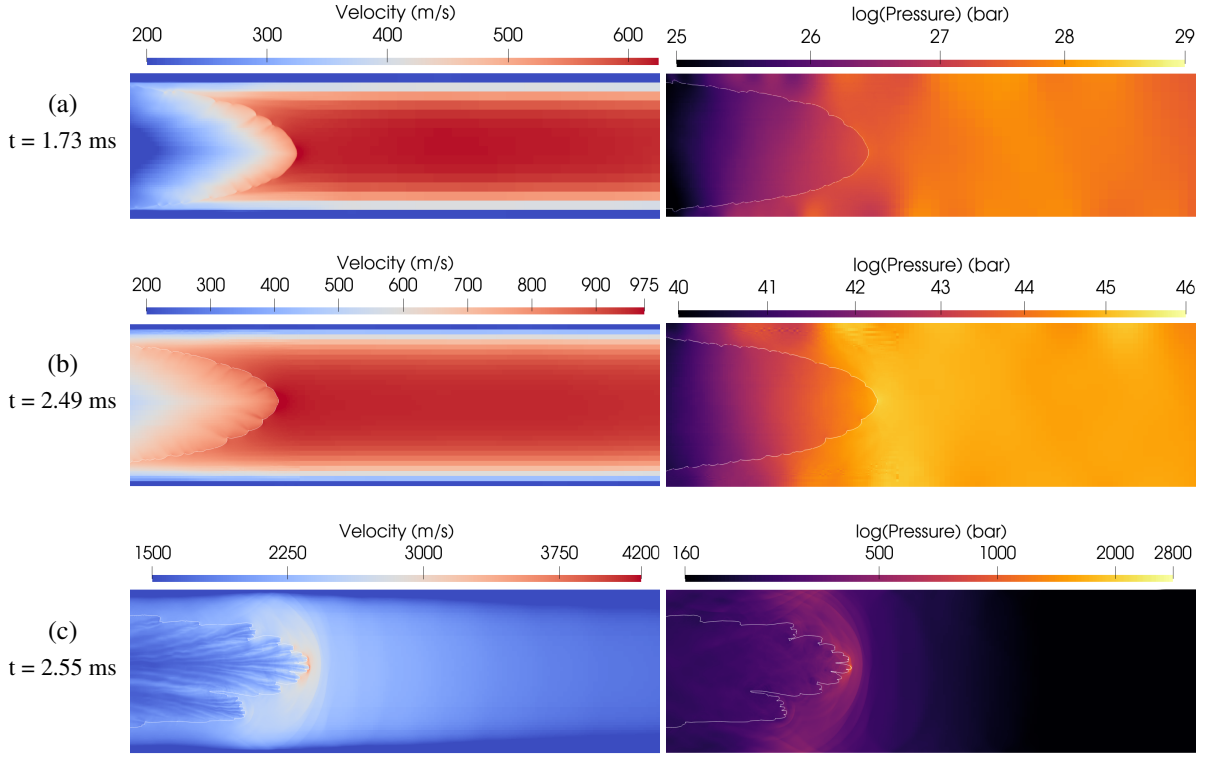

Figure 3: Simulation velocity (left) and pressure (right) fields during the quasi-steady state (1.73 ms), transient (2.49 ms), and detonation onset (2.55 ms).

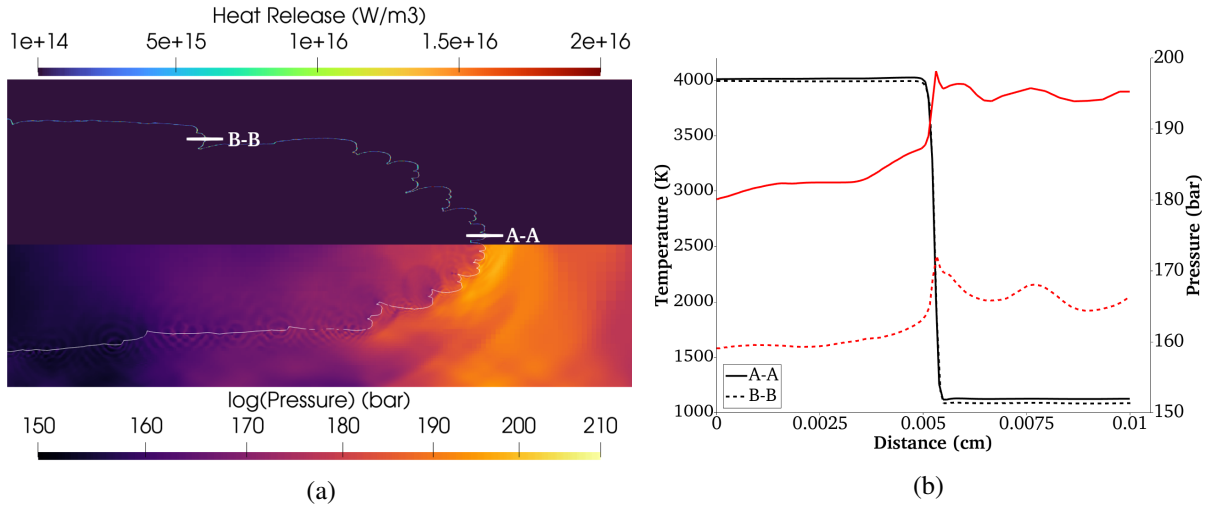

Figure 4: Simulation heat release and pressure fields (left) and spatial variation of temperature and pressure across the flame (right) at the flame tip (solid) and near the wall (dashed) $\sim$ 3.25 μs before DDT.

1.73 ms). Both field variables are uniform in the region ahead of the flame, with an average velocity and pressure of $\sim$ 620 m/s and $\sim$ 28 bar, respectively.

Immediately prior to transition, i.e., $t \approx 2.4$ ms, the dynamics becomes highly transient, resulting in the development of large gradients in the gas velocity and pressure. The runaway process is shown to begin at $\sim$ 2.4 ms, following the start of the exponential growth of u_{uf}, u_{bf}, and P_{f} as seen in Fig. 2b. Figure

3b provides the flow field just prior to DDT ($t = 2.49$ ms). There, spatial gradients in velocity and pressure begin developing, marked by a local pressure peak near the flame tip. As the flame continues to runaway towards DDT, these gradients further steepen, as seen just prior to DDT in Fig. 4a. The transient behavior just prior to DDT is the product of the coupling between A_{f}, u_{bf}, and P_{f}, as seen in Fig. 2b. Figure 4b compares the temperature and pressure across the flame at the flame tip (A-A), the pressure increases 45% across the flame, whereas near the wall (B-B), the pressure increase is 7% across the flame. Similar trends are observed for the gas velocity. Inspection of the flame structure and chemical heat release indicates that the flame remains a deflagration until the onset of local pressure buildup ahead of the flame, as seen in Fig. 4.

Figure 3c displays the flow field at detonation onset ($t = 2.55$). DDT is observed to initiate at the tip of the finger-like flame. Detonation onset follows the local high pressures at the flame tip, due to the backflow of burned gas from the lateral edges towards the tip of the flame. Inspection of the heat release during DDT displays a sudden spike in heat release rate from within the flame. The absence of reactions in the unburnt gas ahead of the flame suggests that DDT is unlikely to be a result of the Zeldovich gradient mechanism. This behavior was observed in all simulations conducted in this study, from level 3 to level 6. These observations stress the importance of the role of burned gas (piston) acceleration.

4 Conclusions

In this study, numerical simulation of a stoichiometric H_2/O_2 mixture in a narrow 2-D channel was performed using detailed chemistry. This allowed for the role of the burned gas (piston) driven flame acceleration on DDT to be investigated. Results showed detonation formation following two phases of flame acceleration: quasi-steady and transient. During the quasi-steady regime ($t \lesssim 2.4$ ms), the flow field ahead of the flame remained uniform. Just prior to runaway and DDT ($t > 2.4$ ms), spatial gradients in gas velocity and pressure adjacent to, and ahead of the flame developed. These gradients appear as a result of the growing flame area, which increases burned gas production and backflow toward the flame tip, causing pressure buildup at the flame tip. The observed behavior seems to be consistent with the recent mechanism proposed by Clavin and Tofaili for quasi-steady flames [12] and later by Clavin accounting for transient effects [13–15].

References

[1] Kailasanath, K. (2000) Review of Propulsion Applications of Detonation Waves. AIAA J. 38

[2] Poludnenko, A. Y., Chambers, J., Ahmed, K., Gamezo, V. N., Taylor, B. D. (2019) A unified mechanism for unconfined deflagration-to-detonation transition in terrestrial chemical systems and type Ia supernovae. Science 366

[3] Shchelkin, K. I., Troshin, Y. K. (1965) Gasdynamics of Combustion. Mono Book Corporation

[4] Zeldovich, Y. B. (1980) Regime classification of an exothermic reaction with nonuniform initial conditions. Combust. Flame 39

[5] Lee, J. H., Knystautas, R., Yoshikawa, N. (1987) Photochemical initiation of gaseous detonations. Acta Astronaut. 5

[6] Liberman, M. A., Ivanov, M. F., Kiverin, A. D., Kuznetsov, M. S., Chukalovsky, A. A., Rakhimova, T. V. Deflagration-to-detonation transition in highly reactive combustible mixtures. Acta Astronaut. 67

[7] Ivanov, M. F., Kiverin, A. D., Liberman, M. A. (2011) Flame acceleration and DDT of hydrogen–oxygen gaseous mixtures in channels with no-slip walls. Int. J. Hydrogen Energ. 36

[8] Ivanov, M. F., Kiverin, A. D., Liberman, M. A. (2011) Hydrogen-oxygen flame acceleration and transition to detonation in channels with no-slip walls for a detailed chemical reaction model. Phys. Rev. E 83

[9] Ivanov, M. F., Kiverin, A. D., Yakovenko, I. S., Liberman, M. A. (2013) Hydrogen–oxygen flame acceleration and deflagration-to-detonation transition in three-dimensional rectangular channels with no-slip walls. Int. J. Hydrogen Energ. 38

[10] Poludnenko, A. Y., Gardiner, T. A., Oran, E. S. (2011) Spontaneous transition of turbulent flames to detonations in unconfined media. Phys. Rev. Lett. 107

[11] Deshaies, B., Joulin G. (1989) Flame-speed sensitivity to temperature changes and the deflagration-to-detonation transition. Combust. Flame. 77

[12] Clavin, P., Tofaili, H. (2021) A one-dimensional model for deflagration to detonation transition on the tip of elongated flames in tubes. Combust. Flame 232

[13] Clavin, P. (2023) One-dimensional mechanism of gaseous deflagration-to-detonation transition. J. Fluid Mech. 974

[14] Clavin, P., (2023) Intrinsic transition mechanism to detonation of gaseous laminar flames in tubes. C. R. Mécanique 351

[15] Clavin, P., (2025) Physics of the transition to detonation of gaseous flames. Eur. Phys. J. Plus 140

[16] Kuznetsov, M., Liberman, M., Matsukov, I. (2010) Experimental Study of the Preheat Zone Formation and Deflagration to Detonation Transition. Combust. Sci. Technol. 182

[17] Ramachandran, S., Srinivasan, N., Wang, Z., Behkish, A., Yang, S. (2023) A numerical investigation of deflagration propagation and transition to detonation in a microchannel with detailed chemistry: Effects of thermal boundary conditions and vitiation. Phys. Fluids 35

[18] Houim, R. W., Gamezo, V. N., Oran, E. S. (2013) Flame Acceleration and Deflagration-to-Detonation Transition of Hydrogen-Oxygen in Microchannels. 34th ICDERS

[19] Sitaraman, H., Yellapantula, S., Henry de Frahan, M. T., Perry, B., Rood, R. Grout, R., Day, M. (2021) Adaptive mesh based combustion simulations of direct fuel injection effects in a supersonic cavity flame-holder. Combust. Flame 232

[20] Li, J., Zhao, Z., Kazakov, A., Dryer, F. L. (2004) An updated comprehensive kinetic model of hydrogen combustion. Int. J. Chem. Kinet. 36

[21] Law, C. K. (2006) Combustion Physics. Cambridge University Press